

## Article

# Experimental Research of the Heat Transfer into the Ground at Relatively High and Low Water Table Levels

Tadas Zdankus , Juozas Vaiciunas  and Sandeep Bandarwadkar

Faculty of Civil Engineering and Architecture, Kaunas University of Technology, Studentu Str. 48, LT-51367 Kaunas, Lithuania; juozas.vaiciunas@ktu.lt (J.V.); sandeep.bandarwadkar@ktu.edu (S.B.)

\* Correspondence: tadas.zdankus@ktu.lt

**Abstract:** During the cold period, the heat transferred through the building's external boundaries to the environment changes the naturally established heat balance between atmospheric air and soil layers. The process of the heat transfer into the ground was investigated experimentally in the cases of the relatively high and low levels of the water table. The first part of each experiment was the research of the heat transfer into the soil from the heating surface. The second part was monitoring the heat dissipation in the ground until the return to the initial natural thermodynamic equilibrium after the heating is intercepted. The heating device was installed into the clay at a one-meter depth, and its surface temperature was kept constant at 20 degrees Celsius. The ground was warmed up in contact with the heating surface. The heat spread to other soil layers and transformed the temperature distribution. A new thermodynamic equilibrium was reached six days after the heating started at an initial temperature of 4.4 degrees Celsius. The intensity of the heat flux density approached a stable value equal to 117.4 W/m<sup>2</sup>, which is required to maintain this thermodynamic equilibrium, as the heat was dissipating in the large volume of the surrounding soil. The heating was turned off, and the natural initial heat balance was reached after two weeks.

**Keywords:** heat transfer into the ground; charge by heat; temperature distribution; heat accumulation; heat dissipation; thermal equilibrium



**Citation:** Zdankus, T.; Vaiciunas, J.; Bandarwadkar, S. Experimental Research of the Heat Transfer into the Ground at Relatively High and Low Water Table Levels. *Buildings* **2023**, *13*, 1272. <https://doi.org/10.3390/buildings13051272>

Academic Editor: Chi-Ming Lai

Received: 3 April 2023

Revised: 4 May 2023

Accepted: 11 May 2023

Published: 12 May 2023



**Copyright:** © 2023 by the authors. Licensee MDPI, Basel, Switzerland. This article is an open access article distributed under the terms and conditions of the Creative Commons Attribution (CC BY) license (<https://creativecommons.org/licenses/by/4.0/>).

## 1. Introduction

In northern countries, the thermal energy required to heat buildings accounts for a significant portion of total energy consumption, typically ranging from 40 to 70% in the cold period. The amount of such energy consumption depends on factors such as the local climate, the source of energy used, the building and the pattern of usage [1,2]. Building heating is a process of increasing the temperature of the structures and indoor air to a desired level, making it warm and comfortable for the occupants, especially in cold weather conditions [3]. However, heating systems require regular maintenance to ensure they are operating efficiently and safely. Neglecting maintenance can result in energy waste, equipment failures and safety hazards [4–6].

One of the most critical factors contributing to building energy demand and thermal comfort is the building envelope [7]. Heat loss through the external surfaces of the building to the environment accounts for a significant amount of energy consumed by a building for a heating process [8,9]. That also affects the thermal balance of the ground beneath and around the building as the soil temperature is lower than that of the heated building. Over time, this process can increase the likelihood of soil settlement or reduce soil stability and particularly clay soils, which affect the foundation of the building and structural stability of the building [10,11]. Due to the continued expansion of the residential building sector, it is necessary to reduce energy consumption and maintain an unchanged temperature profile within the building, imposing specific requirements [12]. Related to this is the study of heat loss through the external boundary of the building, thermal characteristics of the ground

and the dissipation of the heat through the various layers of the soil having a different level of the water table. By understanding and mitigating heat loss through the external surfaces, energy efficiency can be increased to obtain economic and environmental benefits.

The strategy must include an advanced analysis of the heat flux to obtain efficient energy consumption [13–15]. To perform the energy calculation, such as heat loss from the external boundary of the building, and to use the ground as a potential source for heat pump applications, understanding the thermal and deformation properties of the surface and subsurface of the ground system is needed [16,17]. The temperatures of soil layers up to 1 m are sensitive to changes in surface temperature and are called the near-surface zone. The shallow zone surface starts at 2 m and changes seasonally to 7 m. The temperature of the soil layers at a depth of more than 7 m remains almost constant on the surface of the deep zone up to 20 m [18,19]. The moisture content and temperature of the ground surface depend on the air temperature, direct and diffuse short-wave radiation, wind speed, relative humidity, rain and vegetation. Evaporation and the amount of precipitation affect the moisture content of the surface. The exact determination of the surface temperature, for which the changes in ground temperature are considerable, is not so easy [20,21].

The ground is a three-phase material containing solids, air and water. The thermal conductivity of the soil depends on the proportion and heat conductivity of each phase. The ground is characterized by specific properties, such as the mineral composition of the solid phase, the proportion of voids and their spatial distribution and the proportion of water that fills the gaps [22,23]. Due to its loose and porous attributes, the soil cannot be a continuous medium. The amount and state of the moisture content present in the soil significantly affect heat transfer because water has a higher thermal conductivity than soil, meaning that it can conduct heat more easily. Furthermore, the thermal properties of the ground, such as thermal conductivity and specific heat capacity that influence the rate of heat transfer, are affected by different percentages of water content. Heat transfer by conduction dominates in the soil with different moisture content [24–27].

In many analyses, heat loss to the ground has been the subject [28–36]. Depending on the geometry of the building projections and the depth of the foundation, four methods were analyzed to define the heat loss to the ground [28,29]. A novel co-simulation method for building energy modelling with dynamic underground heat transfer was determined [30]. A connection system of various forms of nodes having a foundation slab with a foundation wall was analyzed, and changes in linear heat loss coefficients were performed [31]. In the case of shallow foundation buildings, heat loss was studied from the central part of the building and the area around the external walls. Heat loss was analyzed in modular construction and domes where a shallow foundation had been used [32]. An analytic expression for 3D heat transfer with sinusoidal variation in surface temperature varying with time was analyzed [33]. To determine the heat flux from the surface to the semi-infinite ground, Fourier transforms with the periodic condition were used [34]. A technique was developed using the response factor method to calculate the heat flux [35]. A heat loss through the slab of an Australian house was calculated using the 2D transient method based on the response factor [36].

In the era of energy-saving solutions, existing methods of analysis for heat loss into the ground are still based only on the influence of the average temperature of the external environment. Therefore, the objective of the research was to assess the effect of the water table on heat dissipation through the adjacent layers of soil. The increase in ground temperature is acted upon by heat transferred through the surfaces of the building. However, heat dissipates to the consecutive soil layers. A dynamic thermal equilibrium is reached after a certain interval of time. Heat lost to the ground can also be treated as thermal charging of the soil. Therefore, this research focused on the process of charging and heat dissipation in the soil in dependence on the different levels of the water table.

The heat transfer to water-saturated clay in field conditions has not been sufficiently researched. The investigation was performed on the influence of the water table on the thermal properties of soil, which, in turn, influences the amount of heat dissipation and the

velocity of heat propagation to the adjacent soil layers. The knowledge obtained is suitable for the usage of the ground as a thermal accumulator.

## 2. Experimental Setup and Methodology

The simulation and analyses of the heat transfer through the external partitions of the building to the surrounding environment were performed. The focus was on heat transfer into the ground. It was assumed that a comfortable air temperature was maintained inside the building, and part of the heat was lost through the floor or walls, transferring it to the ground. It disrupted the naturally established initial thermal equilibrium in the soil. The ground was warmed up in contact with the outer surface of the wall or floor of the building. The heat spread to other ground layers. The distribution in the soil temperature transformed. Over time, a new thermodynamic balance was reached. The experiments were performed in field conditions. Each experiment consisted of two parts. The first part was the investigation of the heat transfer into the soil from the heating surface. The second part was the monitoring of the heat dissipation in the ground until the return to the initial natural thermodynamic equilibrium after the heating device was off.

The outside of the building's external partition in contact with the soil was simulated by the heating surface of the experimental setup. The heating cable CTAV-18 was evenly mounted onto the chipboard with a thickness of 0.01 m ( $\delta = 0.01$  m). The heating surface was made from a steel plate. Its length and width were equal to 0.50 m and its thickness was equal to 0.001 m. The thermal insulation layer ( $\delta = 0.1$  m) from polystyrene EPS 70 NEO ( $\lambda = 0.031$  W/(m·K)) was placed on the heating device from above. The equipment was put into the ground at 1 m depth. There was a clay layer. The density  $\rho$ , thermal conductivity  $\lambda$  and specific heat  $c_p$  of the clay at a depth of 1 m ( $h = -1.00$ ) were, respectively, equal to  $\rho = 1800 \div 2200$  kg/m<sup>3</sup>,  $\lambda = 0.5 \div 1.5$  W/(m·K) and  $c_p = 1500 \div 2000$  J/(kg·K) in the case of the moist clay of the water content and equal to 50 ÷ 90% (case I) and  $\rho = 1400 \div 2100$  kg/m<sup>3</sup>,  $\lambda = 1.0 \div 2.0$  W/(m·K),  $c_p = 2100$  J/(kg·K) in the case of the fully saturated clay [37,38] (cases II, III and IV). The values of the mentioned parameters of the soil were taken from literature sources [37,38]. Laboratory tests of the soil samples showed the correspondence of real values with those given.

The sensor of the type TJ1-Pt1000/A ( $-30..180$  °C, three-wire) was used for the temperature measurement. Two thermoresistors were placed at the heating surface from the ground side ( $h = -1.00$  m). The other two were located at a distance of 0.25 m ( $h = -1.25$  m) and 0.50 m ( $h = -1.50$  m) below the heating surface center (Figure 1). In addition, the ground temperature was measured until the depth of 0.50 m. This measurement was performed within 5 m of the side of the heating surface to avoid the effect of charged heat. One temperature sensor was placed at the ground surface ( $h = 0$ ), the second at 0.25 m ( $h = -0.25$  m) and the third at a depth of 0.50 m ( $h = -0.50$ ). The air temperature was measured at 1 m height as well. Measurement data were read and transferred to the computer by Data Logger PT-104 (0.001 °C resolution, 0.015 °C accuracy and temperature ranging from  $-200$  to  $+800$  °C).

The constant temperature ( $T_{set}$ ) of the heating surface was the main task for the experimental setup. The temperature controller ATR244-12ABC was used for that purpose. One more temperature sensor TJ1-Pt1000/A was installed at the heating surface from the ground side to have the input signal for the controller. To operate with higher values of electric current ( $I$ ) and accurately perform the measurement, a discrete (on-off) temperature control method was selected for the research. Voltage ( $V$ ) on the heating cable was measured by a multimeter of ESCORT 3136A type. The specifications for the current and voltage measurement were as follows: the resolution of 100  $\mu$ A; accuracy of 2% for the range of 5 A for AC and resolution of 10 mV; and accuracy of 0.5% for the range of 500 V for AC. The second input channel of this device was used for electric current ( $I$ ) measurement. During the experiments, the power of the heating device was equal to  $P = VI = 375 \pm 10$  W. The average heat flux density ( $q_{av}$ ) was the amount of heat transferred per area unit. Since the controller was discretely switched on and off, each time interval of the connected controller

was found. The corresponding power of the heating was recorded by the usage of the multimeter. Thus, the amount of heating power was calculated. To obtain the average heat flux density for a particular time (hour, day), the calculated heat amount was divided by that time and the area of the heating surface (Equation (1)).

$$q_{av} = \frac{\sum_{i=1}^n P_i t_i}{A t_{set}}, \quad (1)$$

where  $t_{set}$  is the time interval for which the average heat flux density was calculated,  $i$  is the number indicating the specific charge,  $n$  is the number of charges per set time interval,  $t_i$  is the duration of a specific charge and  $A$  is the area of the heating surface ( $A = 0.25 \text{ m}^2$ ).

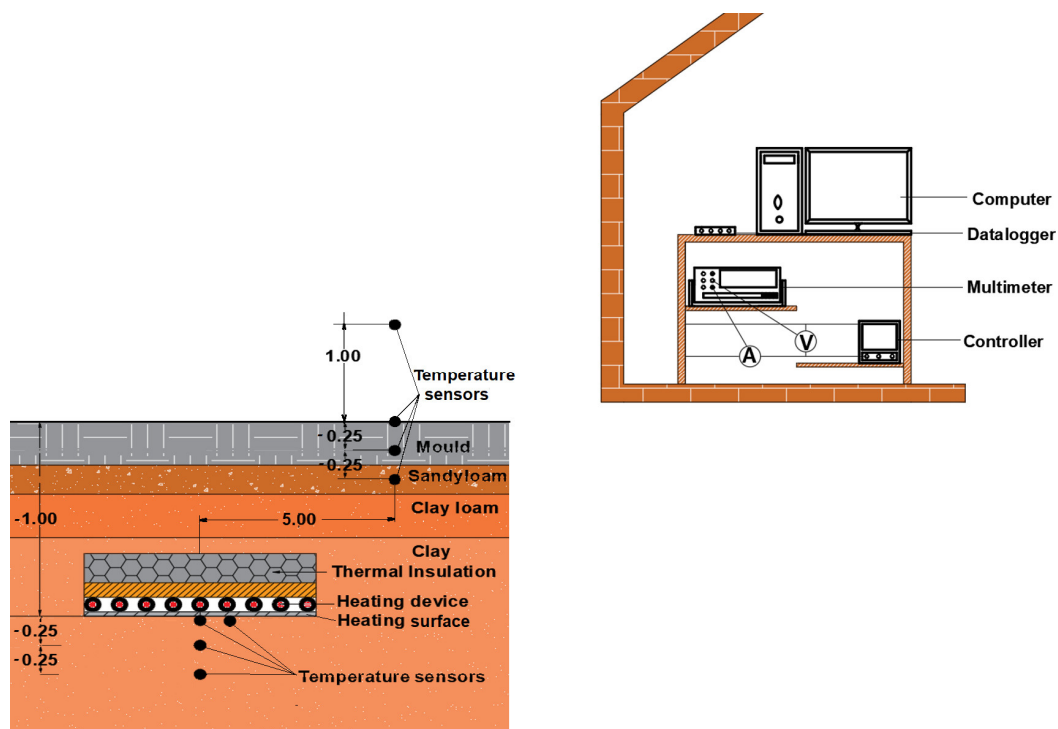


**Figure 1.** Experimental setup.

The consumed electricity was assumed to be equal to the amount of heat generated. The experimental device was composed of components. Therefore, the amount of heat needed to heat each of its components was added up. The total energy ( $Q$ ) used to heat the heating device itself to the  $T_{set}$  temperature was computed by Equation (2) and eliminated from the amount of heat charged into the soil.

$$Q = \sum_{j=1}^k m_j c_{pj} (T_{set} - T_0), \quad (2)$$

where  $Q$  is heat used to warm up the experimental device,  $m$  is the mass,  $c_p$  is specific heat,  $j$  is the number indicating the specific part of the experimental equipment and  $k$  is the number of the parts of the device.

Four experiments, called cases, were performed in total. Research place: Lithuania, Kaunas suburb. The investigation started in 2022 and ended in 2023 and covered the months of December, January and February (Table 1). The dependence of the soil temperature on seasonality was observed: the initial temperature ( $T_0$ ) of the experiments decreased slightly in the winter period (Figure 2). In the first case, the water table ( $h_{wt}$ ) was below the heating surface:  $h_{wt} = -1.60 \text{ m}$ . In the second, third and fourth cases, the water table was above

the heating surface;  $h_{wt} \approx -0.90 \div 1.00$  m. During the research, snow layer formation was episodic and short-lived. Therefore, it was not possible to observe the influence of snow cover on the heat dissipation in the soil.

**Table 1.** Duration of each case (experiment).

Case Number	Heating on	Heating off	End of Experiment
I	9 December	12 December	18 December
II	27 December	1 January	8 January
III	14 January	21 January	5 February
IV	10 February	18 February	5 March

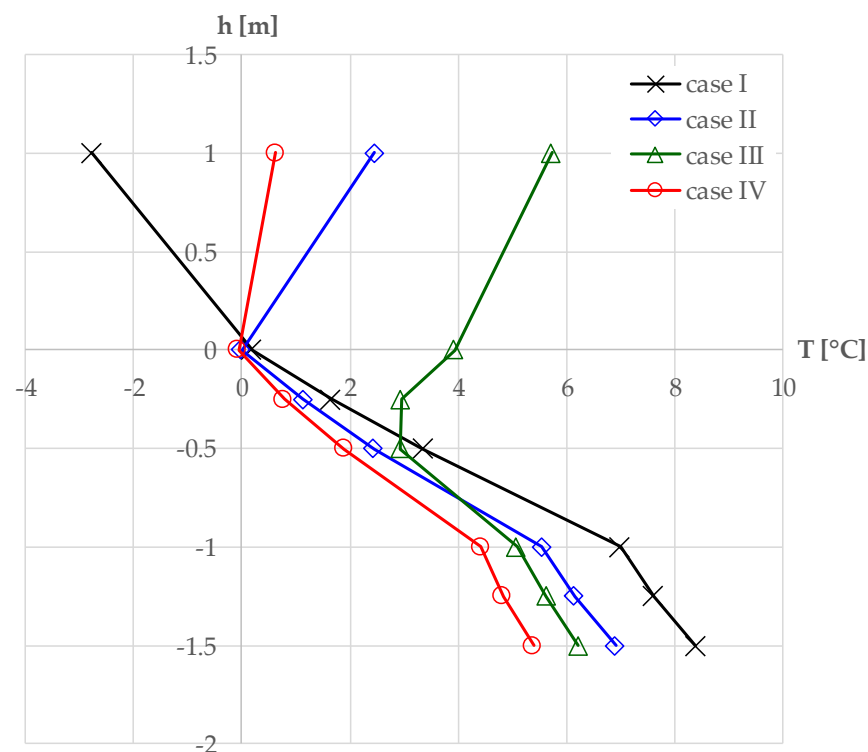


**Figure 2.** Initial temperatures of the soil at different depths in each case.

### 3. Results

The air temperature inside the building should be maintained at 20 degrees Celsius to ensure comfortable conditions throughout the year. During the experiments, the temperature of the air was in the range from  $-2.8$  °C to  $5.7$  °C and the initial temperature of the ground (not deeper than  $-1.50$  m) was in the range from  $-0.1$  °C to  $8.4$  °C (Figure 2). Due to the difference in temperature, heat transfer occurred through the external partitions of the building into the surrounding medium. The research was focused on the analyses of heat transfer into the ground through the imaginary floor or deepened parts of the walls of the building. The temperature of the building's outside surface or the ground there should be known in order to compute the amount of heat loss. It seemed easy to do; however, the heat transfer into the soil warmed the ground and increased the temperature of the ground layer at the contact place. Moreover, many parameters of each layer of the building's partition and the soil, such as the material type, thickness, value of thermal conductivity coefficient, specific heat and humidity in the case of the ground, need to be defined. The natural distribution of the ground temperatures depending on the depth in different seasons should be known.

Some vertical holes at a distance of ten meters from the heating surface were drilled to measure the water table level. The colored indicator was put into one of the holes. The appearance of the indicator in another hole allowed us to find the approximate velocity of the water in the soil, which was almost equal to zero.

There was a natural distribution in the temperature of the soil before the experiment started (Figure 2). A higher temperature of the heating surface, which was equal to 20 degrees Celsius, was set to increase the difference in temperature. The controller's connection to the electricity meant the start of the experiment. The controller worked discretely. It was turning the heating surface on at  $T_{set} = 20$  °C and was turning it off at 20.2 °C.

At the beginning of the experiment of each case, after the regulator connected the heating element to electricity, part of the energy was spent on heating the element itself and the surfaces of the equipment in contact with it. As a result, a slight delay in the change in soil temperature was observed at the heating surface place at the depth of 1 m. The increased temperature of the heating surface acted on the heat transfer from it into the colder ground. A layer of the soil near the surface was heated, and at the same time, heat transfer proceeded from it to further soil layers and so on.

The experimental equipment were heated from the initial temperature, equal to ground temperature ( $T_0$ ), at  $-1$  m depth to the set temperature ( $T_{set}$ ). Energy was computed by knowing the volume and the density or the mass and heat capacity of each component of the heating device (Equation (2)), and this amount was eliminated from the value of the first thermal charge. After the heating surface's temperature reached 20 degrees Celsius, it was assumed that the consumed electricity was fully converted into heat and charged into the soil. Therefore, it was assumed that at a short distance from the heating surface (in  $0.25 \div 0.50$  m), the main part of the heat spread downwards and another part of it to the sides. Initially, the energy was used to heat up the soil layer closest to the heating surface. Next, the heat transferred from the bit-heated layer to the others and so on. The impact of such heating on the soil properties and its deformations was insignificant and has not yet been discussed.

The difference in temperature between the heating surface and the nearest ground layer increased until the temperature of the heating surface reached a set value ( $T_{set}$ ) and was kept constant. The highest heat amount was charged into the soil at the beginning of the experiment. It decreased evenly as the ground warmed up and thermal energy was needed to compensate for the heat transfer to other soil layers below or to the sides. The most intense average heat flux density was observed in the first hour (Figure 3). It was 2.3 times higher than the heat flux density at the second hour in the first case ( $q_{av,1h}/q_{av,2h} = 2.3$ ), three times in case II, 2.7 times in case III and 2.6 times in case IV. During the first hour, 13.5–15.7% of the total amount of thermal energy of the first day was charged into the ground (Figure 4) and, accordingly, 5.3–6.0% in the second hour, 4.5–4.9% in the third, 4.3–4.5% in the fourth hour and less than 4.2%, with a decreasing character, in the following hours (Figure 4).

Two influencing factors were identified by analyzing the results of different cases (Figures 3 and 5). The initial temperature of the soil ( $T_0$ ) was one of them. In the first case, at the 1 m depth from the heating surface, the initial temperature of the ground was equal to  $T_{0,I} = 7.0$  °C and, accordingly,  $T_{0,II} = 5.5$  °C for case II,  $T_{0,III} = 5.1$  °C for case III and  $T_{0,IV} = 4.4$  °C for case IV (Figure 2). As was mentioned above, the set temperature of the heating surface was equal to  $T_{set} = 20$  °C. Therefore, the difference in temperatures ( $\Delta T = T_{set} - T_0$ ) was not the same at the beginning of the experiment for each case.  $\Delta T$  was equal to  $\Delta T_I = 13.0$  °C for case I,  $\Delta T_{II} = 14.5$  °C for case II,  $\Delta T_{III} = 14.9$  °C for case III and  $\Delta T_{IV} = 15.6$  °C for case IV. The heat amount required to heat colder soil should be higher than that for soil with a higher initial temperature. It would be concluded that the highest amount of thermal energy was charged into the ground in case IV. It would be less in cases III and II and the least in case I. Analysis of the results shows that the most intensive heat flux density was in case III ( $q_{av,h,III} = 646.3$  W/m<sup>2</sup>) and less in cases

IV ( $q_{av,h,IV} = 615.3 \text{ W/m}^2$ ) and II ( $q_{av,h,II} = 591.1 \text{ W/m}^2$ ) in the first hour. In the first case, the intensity of the heat flux density differed greatly from the mentioned three cases and was equal to  $q_{av,h,I} = 430.7 \text{ W/m}^2$ . This tendency remained throughout the three days, although the difference between the  $q_{av,h}$  values was not so significant (Figure 5). After three days, the heat flux density of case IV became slightly higher than that of case III.

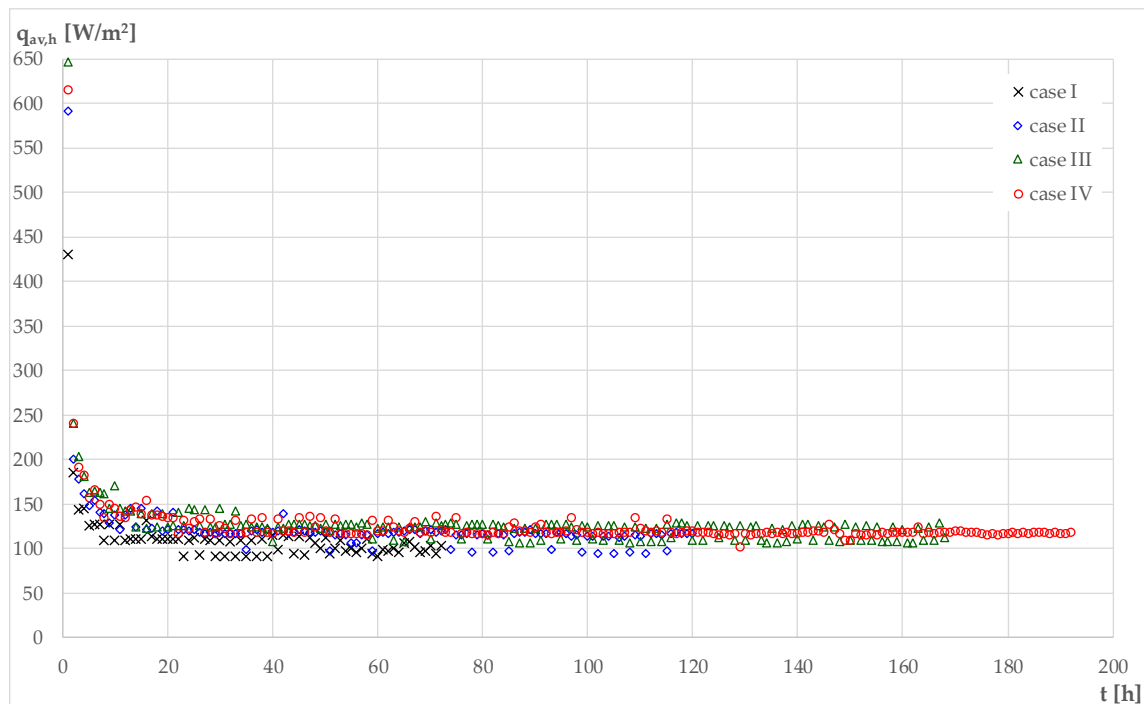


Figure 3. Change in the average hourly heat flux density of the heat transfer into the ground.

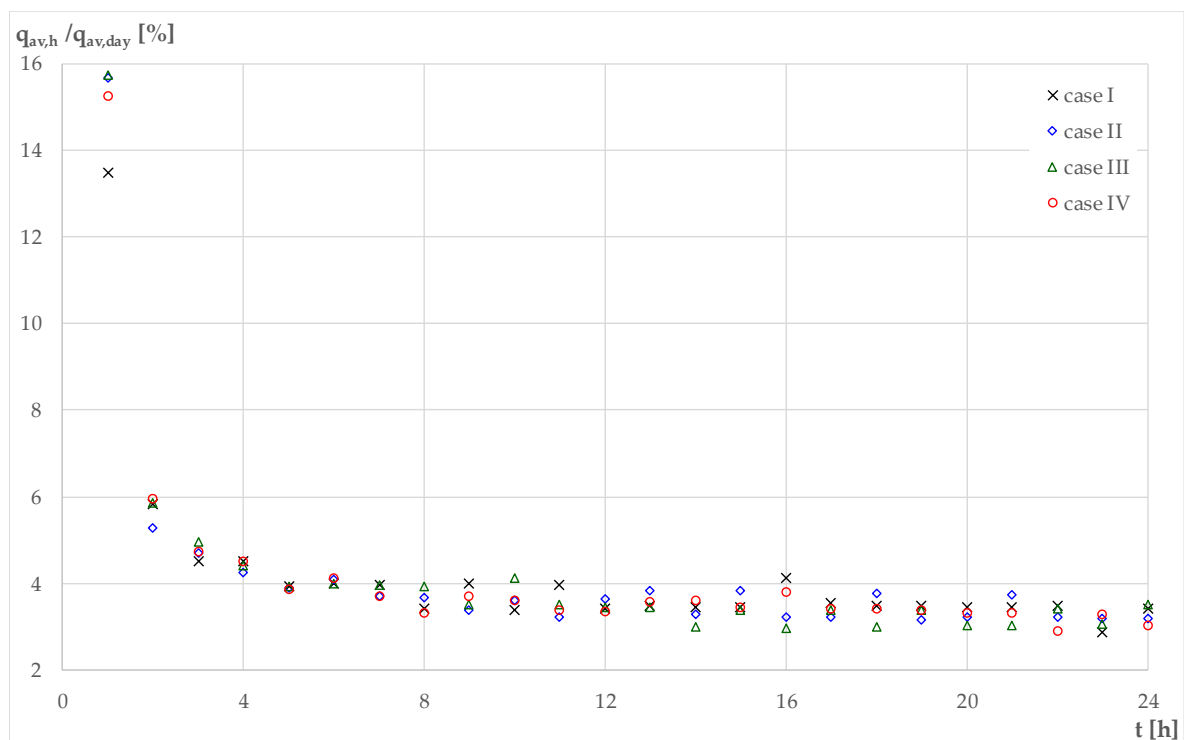
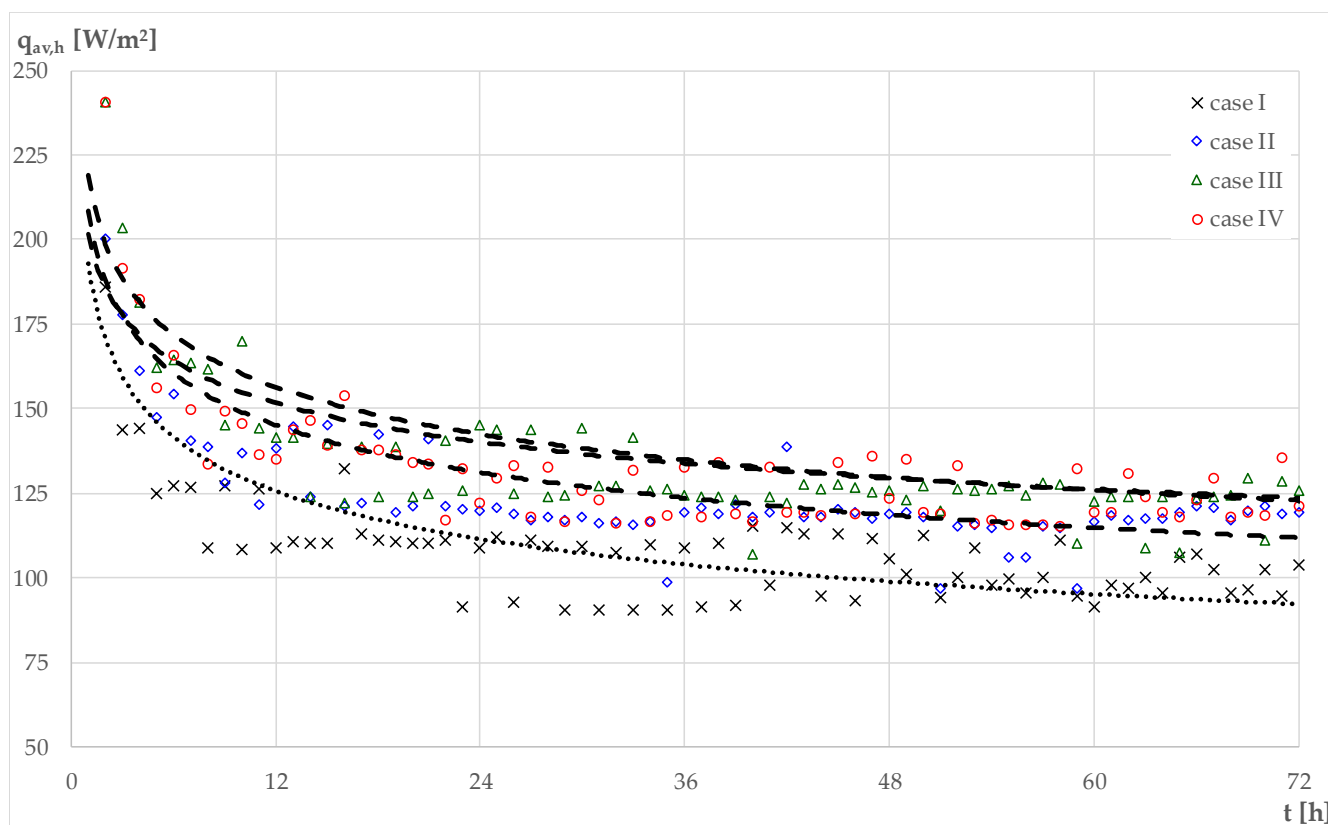


Figure 4. The relative change in the intensity of the heat flux density in the period of the first day.



**Figure 5.** Change in the average hourly heat flux density of the heat transfer into the ground. The interval of time is three days, starting from the second hour. Round dotted line—case I; dashed line—cases II, III and IV (high level of the water table).

The average daily values of heat flux density  $q_{av,day}$  were computed and shown in Figure 6. The function had the same character as discussed previously. The first case significantly differed from the others. This phenomenon cannot be explained only by the difference in initial temperatures ( $T_0$ ). Here, the influence of the water table was observed. In the case of high water table levels (cases II, III and IV), the ground was saturated with water and had a higher value of the specific heat. Therefore, more heat was needed to warm it up. From a technical viewpoint, this would create the possibility to charge higher amounts of heat per unit volume of the soil. Since the value of the thermal conductivity coefficient  $\lambda$  increased as well, the charging itself could be performed more intensively. However, it should be noted that the heat would also spread faster to other layers of the soil and lose the thermal accumulation properties. In the case of groundwater flow, the flow would carry away the greater amount heat.

The velocity of heat propagation can be defined by the time interval between the heating being turned and the reaction of the temperature sensor placed at the distance (Figure 7). In our research, it meant the change in the value of the temperature measured at a depth of  $-1.25$  m ( $\Delta l = 0.25$  m). The temperature started to change after  $t_{1.25,I} = 1$  h 22 min 41 s (4961 s) in case I. The heat reached the deeper sensor later. Therefore, the temperature kept the same value at the depth equal to  $h = -1.50$  m for the time interval given in Figure 7. Accordingly,  $t_{1.25}$  was equal to  $t_{1.25,II} = 1$  h 12 min 35 s (4355 s) in case II,  $t_{1.25,III} = 58$  min 36 s (3516 s) in case III and  $t_{1.25,IV} = 1$  h 22 min 13 s (4933 s) in case IV. In case I, heat covered the distance of  $\Delta l = 0.25$  m 11 min 29 s slower than that in other cases. This phenomenon can be explained by the increased thermal conductivity in the case of fully saturated soil, which allowed a 16% faster soil charge by heat. The temperature change was observed after  $t_{1.50,I} = 6$  h 47 min 20 s (24,440 s) at the depth of  $-1.50$  m in case I. In case II, it took less time and  $t_{1.50}$  was equal to  $t_{1.50,II} = 6$  h 11 min 11 s (22,271 s) and, respectively,

$t_{1.50,III} = 6 \text{ h } 17 \text{ min } 3 \text{ s } (22,623 \text{ s})$  and  $t_{1.50,IV} = 5 \text{ h } 54 \text{ min } 30 \text{ s } (21,270 \text{ s})$  in cases III and IV. In the case of high water table level, the heat reached the sensor on average about 40 min or 11% earlier than in case I. This phenomenon can be explained by less temperature difference between adjacent soil layers at higher depths, the heat dissipation to the sides and the heat carried off by groundwater flow. This also explained the decrease in the velocity of heat propagation at a greater distance from the heating surface.

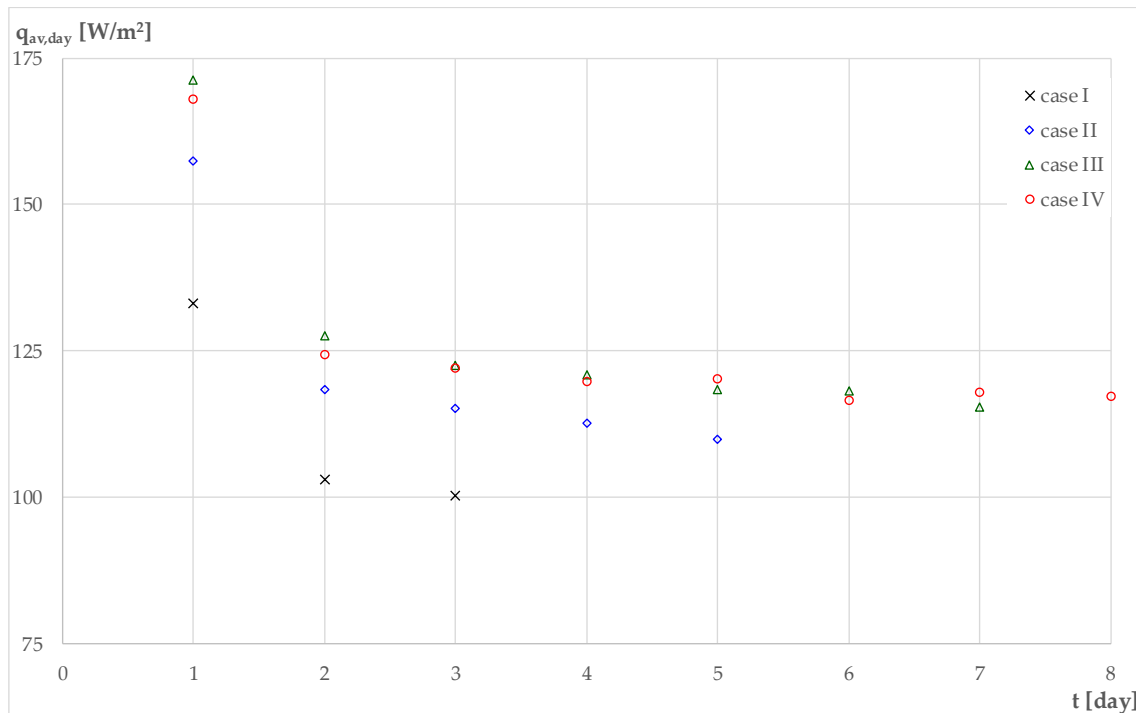


Figure 6. Change in the average daily heat flux density of the heat transfer into the ground.

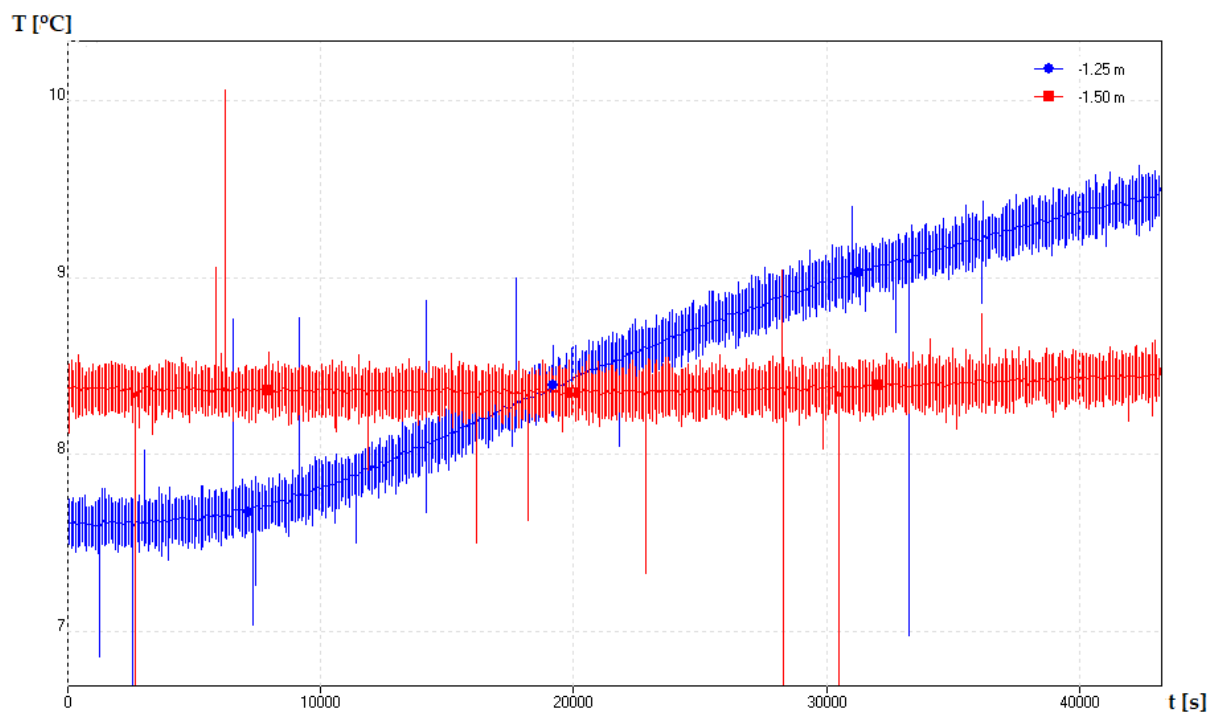
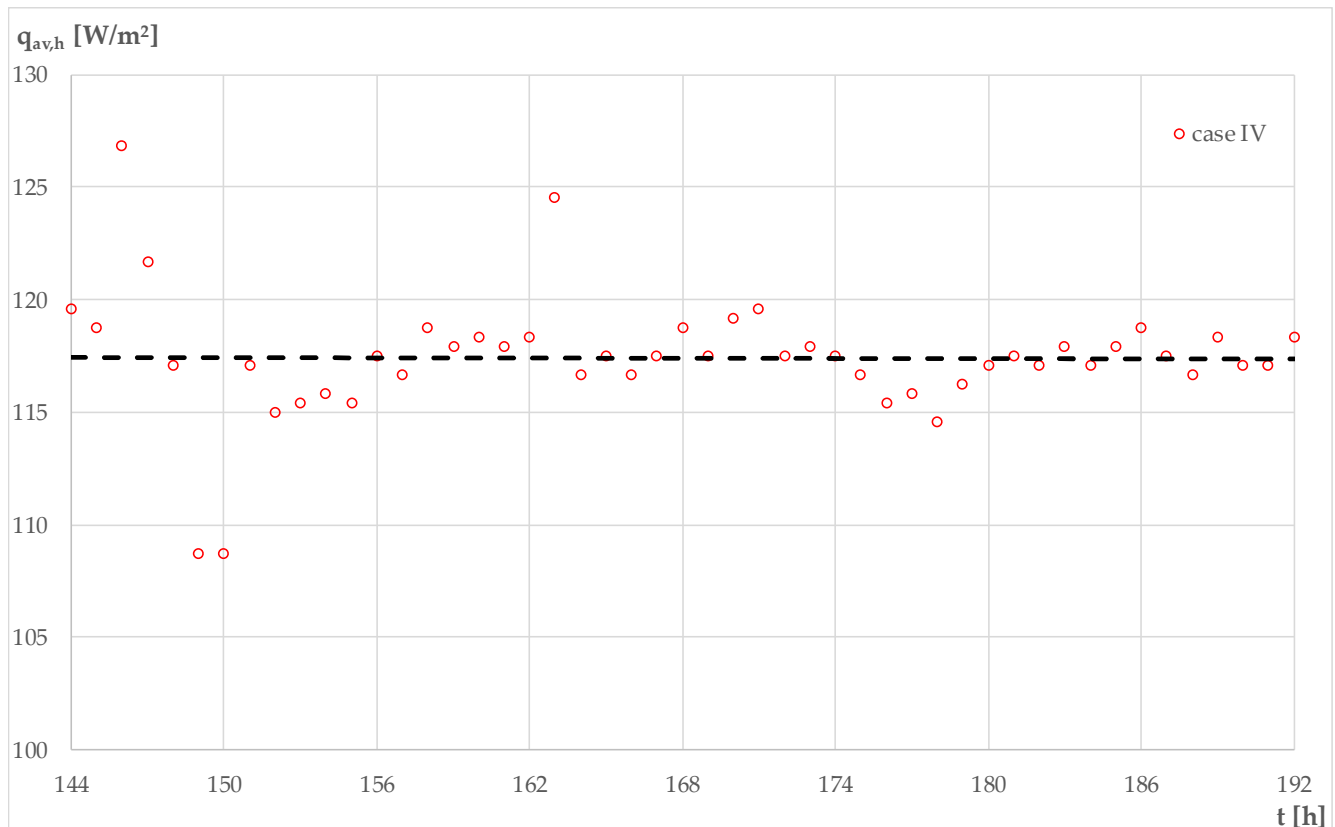


Figure 7. Change in temperature at the depths  $-1.25 \text{ m}$  and  $-1.50 \text{ m}$  in case I. Heating is turned on.

After a time interval, the almost-constant temperature value steadied in the depths of  $-1.25$  m and  $-1.50$  m. The value of the heat flux density was also not changing. It meant that the dynamic thermal balance was reached. The energy of the heating equipment was used fully to compensate for the heat dissipation in the soil. The experiment was aimed to determine the time during at which this state was steadied and to find the value of the heat flux density. Experimental case IV was devoted to this. It was noticed that the thermal balance was reached after six days. On the eighth day, the average hourly heat flux density ( $q_{av,h}$ ) remained constant and equal to  $q_{av,h} = 117.4$  W/m<sup>2</sup> (Figure 8).



**Figure 8.** Change in the average hourly heat flux density on the seventh and eighth days.

After turning off the heating, the temperature of the heating surface fell immediately. The constant value of the temperature remained for a certain period, after which a decrease in temperature was observed at the depths of  $-1.25$  and  $-1.50$  m (Figure 9). Due to the pulsations of the measured value of the temperature, it was difficult to determine at which moment the temperature started to change. The time was measured from the moment the heating was turned off. The temperature started to change at the latest in case I at a depth of  $1.25$  m— $t_{1.25,I} = 1$  h 58 min 7 s (7087 s) from  $T_{1.25,I} = 10.9$  °C—and at a depth of  $-1.50$  m— $t_{1.50,I} = 8$  h 46 min 46 s (31,606 s) from  $T_{1.50,I} = 9.2$  °C. Other time values were measured and are presented in Table 2.

After turning off the heating, the heat spread continued. It was waiting for the natural temperature distribution to settle down. The temperature changes ( $\Delta T = T_{24:00} - T_{00:00}$ ) during each day at the same depths ( $-1$  m,  $-1.25$  m and  $-1.50$  m) were found and are presented in Table 3. In the first two cases, heat dissipation was observed for about a week; later, the time was extended to two weeks (cases III and IV). Slower heat dissipation was observed in case I.

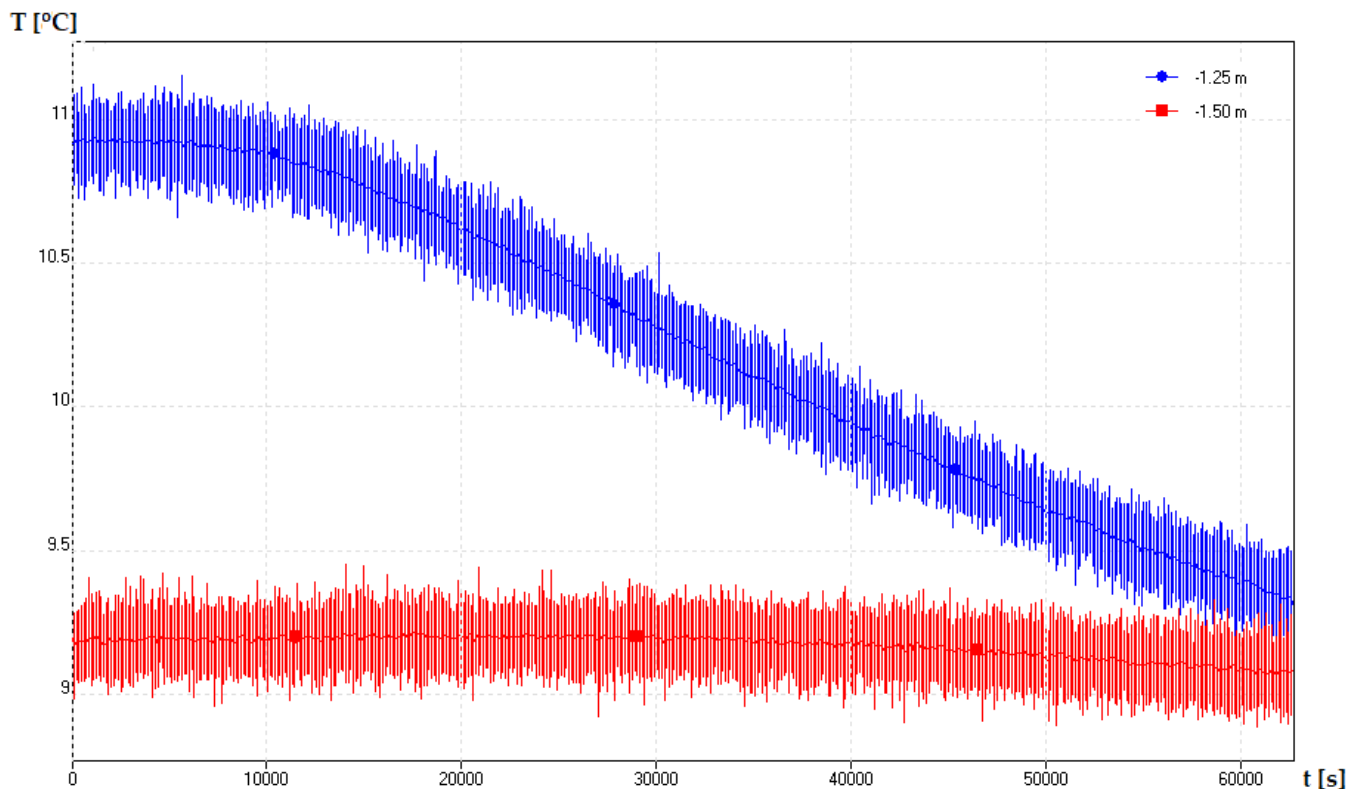


**Figure 9.** Change in temperature at the depths  $-1.25$  m and  $-1.50$  m in case I. Heating is turned off.

**Table 2.** Time interval until the temperature started to decrease at the depths of  $-1.25$  m and  $-1.50$  m after the heating was turned off.

Case Number	$t_{1.25}$ , h, min, s	$t_{1.25}$ , s	$T_{1.25}$ , °C	$t_{1.50}$ , h, min, s	$t_{1.50}$ , s	$T_{1.50}$ , °C
I	1 h 58 min 7 s	7087	10.9	8 h 46 min 46 s	31,606	9.2
II	1 h 56 min 36 s	6996	10.0	8 h 40 min 27 s	31,227	8.0
III	1 h 46 min 55 s	6415	9.8	8 h 26 min 35 s	30,395	7.6
IV	1 h 47 min 55 s	6475	9.0	8 h 27 min 39 s	30,459	6.9

The heat stored in the ground near the heating surface had a higher temperature than in the adjacent soil layers. Therefore, it spread to the colder soil layers and did not allow them to cool down quickly. It was most noticeable at  $-1.5$  m depth on the first day (Table 3). The highest temperature difference ( $\Delta T_{1.50}$ ), indicating the highest heat loss into the soil layers below, was observed on the second day.

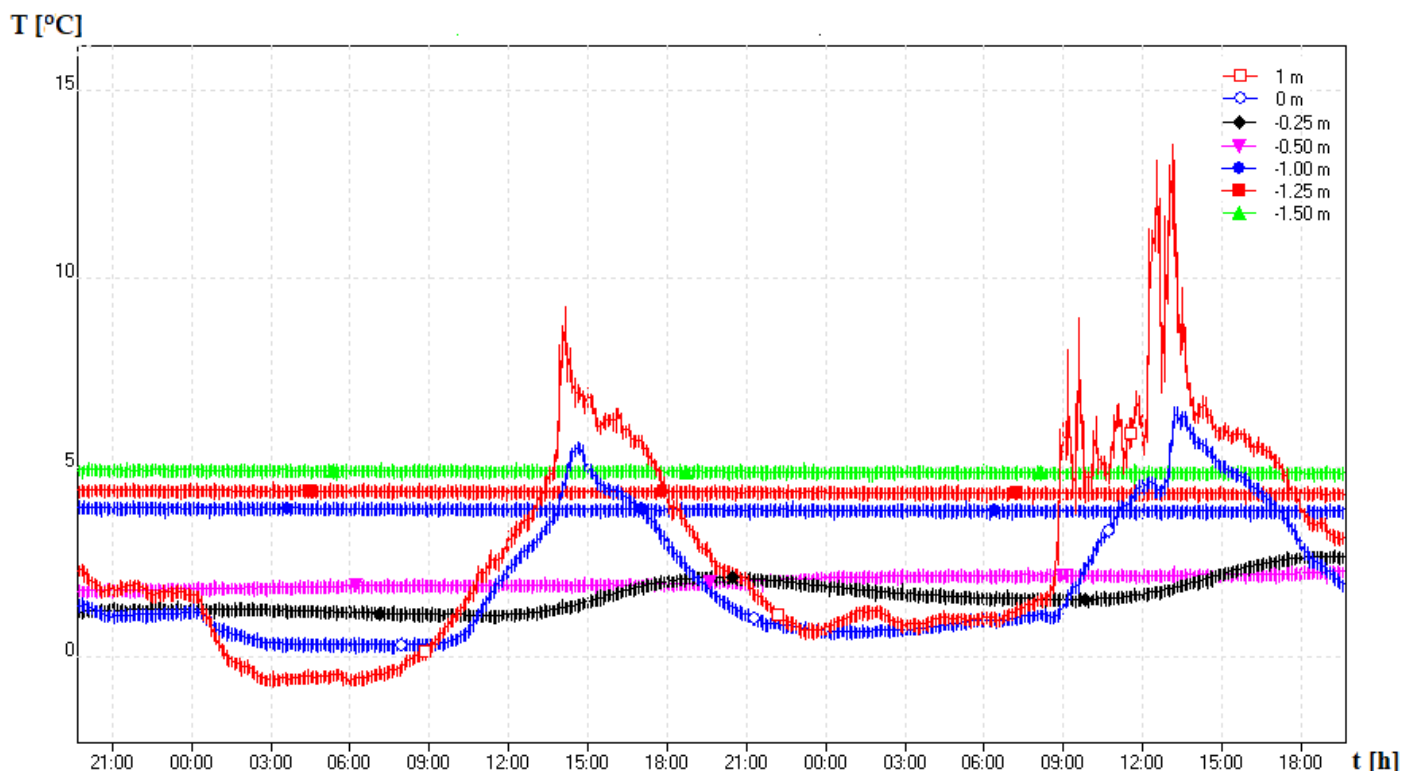
The stored heat dissipated in about two weeks, and it achieved the naturally formed temperature distribution in the soil.

Only the influence of seasonality on soil temperatures at a depth higher than 1 m was monitored (Figure 2) during the experiments. However, in the daytime, the impact of the higher change in air temperature and solar radiation on the soil surface and the ground layers was observed at depths of  $-0.25$  m and  $-0.50$  m (Figure 10).

We researched the heat transfer from the heating surface to the layer of the water-saturated clay at the depth of 1 m. The heat flux was directed downward, and the change in the temperature was analyzed only in the short vertical distance from the surface; the heat dissipation to other directions was not researched.

**Table 3.** Daily temperature difference at the depths of  $-1.00$  m,  $-1.25$  m and  $-1.50$  m.

Case	$\Delta T_i$ , °C	1 Day	2 Day	3 Day	4 Day	5 Day	6 Day	7 Day	8 Day	9 Day	10 Day	11 Day	12 Day	13 Day	14 Day	15 Day
I	$\Delta T_{1.00}$	10.97	1.02	0.41	0.30	0.16	0.18									
	$\Delta T_{1.25}$	2.14	0.81	0.45	0.15	0.19	0.23									
	$\Delta T_{1.50}$	0.21	0.50	0.28	0.22	0.06	0.15									
II	$\Delta T_{1.00}$	12.18	1.09	0.29	0.11	0.14	0.17	0.07								
	$\Delta T_{1.25}$	2.29	0.95	0.24	0.10	0.14	0.12	0.10								
	$\Delta T_{1.50}$	0.31	0.46	0.16	0.18	0.07	0.02	0.11								
III	$\Delta T_{1.00}$	11.57	1.28	0.52	0.26	0.24	0.13	0.11	0.16	0.07	0.17	0.00	0.10	0.12	0.05	0.10
	$\Delta T_{1.25}$	2.14	0.99	0.44	0.34	0.14	0.12	0.20	0.06	0.09	0.07	0.04	0.07	0.13	0.00	0.14
	$\Delta T_{1.50}$	0.32	0.52	0.30	0.15	0.15	0.15	0.04	0.13	0.08	0.02	0.10	-0.01	0.14	0.05	0.06
IV	$\Delta T_{1.00}$	12.24	1.26	0.48	0.30	0.19	0.14	0.17	0.05	0.18	0.02	0.12	0.01	0.07	-0.10	0.05
	$\Delta T_{1.25}$	2.16	0.97	0.43	0.36	0.08	0.19	0.11	0.11	0.04	0.18	0.05	-0.04	0.03	0.08	0.05
	$\Delta T_{1.50}$	0.34	0.47	0.35	0.18	0.12	0.11	0.15	0.01	0.05	0.13	0.09	-0.03	0.14	0.00	-0.05

**Figure 10.** Change in temperature at the different depths in case IV. Heating is turned off.

#### 4. Conclusions

This research was focused on heat transfer into the soil. The ground charging by the heat, the heat dissipation and the formation of the thermodynamic equilibrium were observed and analyzed. The results obtained in the research may be applied in the preparation of soil for the intensive dissipation of the surplus heat of hybrid solar modules, solar collectors or other devices, and the heat may accumulate for later use.

A high level of the water table led to water-saturated soil with higher values of specific heat and thermal conductivity and more intensive heat transfer. The average hourly heat flux density was equal to  $618 \text{ W/m}^2$  for the first hour. In the case of the low water table level, it was less ( $431 \text{ W/m}^2$ ). During the first hour, 13.5–15.7% of the total amount of thermal energy on the first day was charged into the ground and, accordingly, 5.3–6.0% in the second hour, 4.5–4.9% in the third hour, 4.3–4.5% in the fourth hour and less than 4.2%, with a decreasing character, in the following hours.

The new dynamic thermal balance was reached six days after the heating started at the initial temperature of 4.4 degrees Celsius. The temperature of the heating surface was

kept constant at 20 degrees Celsius. The heat from the experimental equipment completely covered the heat dissipation in the fully saturated clay at  $-1$  m depth. The steady value of the average hourly heat flux density was equal to  $117.4$  W/m<sup>2</sup>. It took two weeks to reach the initial thermal balance after the heating was turned off.

It is appropriate to use the soil as a thermal accumulator for the heat exchange. For that purpose, a certain volume of the soil needs to be separated and thermoinsulated from the whole. Further research should focus on the impact of soil thermal charge and discharge on the ground temperature distribution and the soil's ability to retain the heat over a longer period.

**Author Contributions:** Conceptualization, T.Z.; methodology, T.Z., J.V. and S.B.; validation, T.Z., J.V. and S.B.; formal analysis, T.Z., J.V. and S.B.; investigation, T.Z., J.V. and S.B.; resources, T.Z., J.V. and S.B.; data curation, T.Z. and J.V.; writing—original draft preparation, T.Z., J.V. and S.B.; writing—review and editing, T.Z., J.V. and S.B.; visualization, T.Z., J.V. and S.B.; supervision, T.Z. All authors have read and agreed to the published version of the manuscript.

**Funding:** This research received no external funding.

**Data Availability Statement:** Data used in the paper is available in the KTU Faculty of Civil Engineering and Architecture, in the data archive of the experimental research of geothermal properties (tadas.zdankus@ktu.lt).

**Conflicts of Interest:** The authors declare no conflict of interest.

## References

- Zaharia, A.A.; Diaconeasa, M.C.; Brad, L.; Lădaru, G.R.; Ioanăs, C. Factors influencing energy consumption in the context of sustainable development. *Sustainability* **2019**, *11*, 4147. [\[CrossRef\]](#)
- Penttinen, P.; Vimpri, J.; Junnila, S. Optimal seasonal heat storage in a district heating system with waste incineration. *Energies* **2021**, *14*, 3522. [\[CrossRef\]](#)
- Ayanlade, A.; Esho, O.M.; Popoola, K.O.; Jeje, O.D.; Orola, B.A. Thermal condition and heat exposure within buildings: Case study of a tropical city. *Case Stud. Therm. Eng.* **2019**, *14*, 100477. [\[CrossRef\]](#)
- Ormandy, D.; Ezratty, V. Thermal Discomfort and Health: Protecting the Susceptible from Excess Cold and Excess Heat in Housing. *Adv. Build. Energy Res.* **2016**, *10*, 84–98. [\[CrossRef\]](#)
- Lamsal, P.; Bajracharya, S.B.; Rijal, H.B. A Review on Adaptive Thermal Comfort of Office Building for Energy-Saving Building Design. *Energies* **2023**, *16*, 1524. [\[CrossRef\]](#)
- Jamaludin, N.; Mohammed, N.I.; Khamidi, M.F.; Wahab, S.N.A. Thermal Comfort of Residential Building in Malaysia at Different Micro-climates. *Procedia* **2015**, *170*, 613–623. [\[CrossRef\]](#)
- Shao, E.C. Detecting Sources of Heat Loss in Residential Buildings from Infrared Imaging. Ph.D. Thesis, Massachusetts Institute of Technology, Cambridge, MA, USA, 2011. [\[CrossRef\]](#)
- Paukštys, V.; Cinelis, G.; Mockienė, J.; Daukšys, M. Airtightness and heat energy loss of mid-size terraced houses built of different construction materials. *Energies* **2011**, *14*, 6367. [\[CrossRef\]](#)
- Sobota, T.; Taler, J. Determination of heat losses through building partitions. In Proceedings of the XI International Conference on Computational Heat, Mass and Momentum Transfer (ICCHMT 2018), Kraków, Poland, 21–24 May 2018. [\[CrossRef\]](#)
- Mammadov, N.Y.; Akbarova, S.M. Analysis of Thermal Stability of Wall Enclosing Structure of Building for Climatic Conditions. *Int. J. Tech. Phys. Probl. Eng.* **2022**, *50*, 136–141.
- Kelishadi, H.; Mosaddeghi, M.R.; Ayoubi, S.; Mamedov, A.I. Effect of temperature on soil structural stability as characterized by high energy moisture characteristic method. *Catena* **2018**, *170*, 290–304. [\[CrossRef\]](#)
- Dyussebekova, N.; Temirgaliyeva, N.; Umyshev, D.; Shavdinova, M.; Schuett, R.; Bektalieva, D. Assessment of Energy Efficiency Measures' Impact on Energy Performance in the Educational Building of Kazakh-German University in Almaty. *Sustainability* **2022**, *14*, 9813. [\[CrossRef\]](#)
- Ma, J.J.; Du, G.; Xie, B.C.; She, Z.Y.; Jiao, W. Energy Consumption Analysis on a Typical Office Building: Case Study of the Tiejian Tower, Tianjin. *Energy Procedia* **2015**, *75*, 2745–2750. [\[CrossRef\]](#)
- Ploennigs, J.; Menzel, K. Analyze building performance data for energy-efficient building operation. In Proceedings of 26th W78 Conference on Information Technology in Construction, Istanbul, Turkey, 1–3 October 2009.
- Umbark, M.A.; Alghoul, S.K.; Dekam, E.I. Energy Consumption in Residential Buildings: Comparison between Three Different Building Styles. *Sustain. Dev. Res.* **2020**, *2*, 1–8. [\[CrossRef\]](#)
- Usonicz, B. A Method for the Estimation of Thermal Properties of Soil. *Int. Agrophys* **1993**, *1*, 27–34.
- Shonder, J.A.; V Beck, J. *A New Method to Determine the Thermal Properties of Soil Formations from In Situ Field Tests*; Technical Report; U.S. Department of Energy Office of Scientific and Technical Information: Oak Ridge, TN, USA, 1996; pp. 1–40. [\[CrossRef\]](#)

18. Pokorska-Silva, I.; Kadela, M.; Orlik-Ko, B.; Fedorowicz, L. Calculation of Building Heat Losses through Slab-on-Ground Structures Based on Soil Temperature Measured In Situ. *Energies* **2022**, *15*, 114. [[CrossRef](#)]
19. Popiel, C.O.; Wojtkowiak, J.; Biernacka, B. Measurements of temperature distribution in ground. *Exp. Therm. Fluid Sci.* **2001**, *25*, 301–309. [[CrossRef](#)]
20. Larwa, B. Heat transfer model to predict temperature distribution in the ground. *Energies* **2019**, *12*, 25. [[CrossRef](#)]
21. Yu, J.; Kang, Y.; Zhai, Z. Comparison of ground coupled heat transfer models for predicting underground building energy consumption. *J. Build. Eng.* **2020**, *32*, 101808. [[CrossRef](#)]
22. Salata, F.; Falasca, S.; Ciancio, V.; Curci, G.; Grignaffini, S.; Wilde, P. Estimating building cooling energy demand through the Cooling Degree Hours in a changing climate: A modeling study. *Sustain. Cities Soc.* **2022**, *76*, 103518. [[CrossRef](#)]
23. Pouloupatis, P.D.; Florides, G.; Tassou, S. Measurements of ground temperatures in Cyprus for ground thermal applications. *Renew. Energy* **2011**, *36*, 804–814. [[CrossRef](#)]
24. Kasubuchi, T. The effect of soil moisture on thermal properties in some typical Japanese upland soils. *Soil Sci. Plant Nutr.* **1975**, *21*, 107–112. [[CrossRef](#)]
25. Cosenza, P.; Guerin, R.; Tabbagh, A. Relationship between thermal conductivity and water content of soils using numerical modelling. *Eur. J. Soil Sci.* **2003**, *54*, 581–587. [[CrossRef](#)]
26. Roxy, M.S.; Sumithranand, V.B.; Renuka, G. Estimation of soil moisture and its effect on soil thermal characteristics at Astronomical Observatory, Thiruvananthapuram, south Kerala. *J. Earth Syst. Sci.* **2014**, *123*, 1793–1807. [[CrossRef](#)]
27. Park, M. A Study on Heat-Transfer Characteristics by a Ground-Heating Method. *Sustainability* **2018**, *10*, 412. [[CrossRef](#)]
28. Saaly, M.; Maghoul, P.; Holländer, H. Investigation of the effects of heat loss through below-grade envelope of buildings in urban areas on thermo-mechanical behaviour of geothermal piles. In Proceedings of the 2nd International Conference on Energy Geotechnics (ICEGT 2020), La Jolla, CA, USA, 10–13 April 2022. [[CrossRef](#)]
29. Khalifa, A.J.N. Heat loss from below ground basements: Validation of some available methods. *Energy Convers. Manag.* **1999**, *40*, 1963–1977. [[CrossRef](#)]
30. Kang, X.; Yan, D.; Xie, X.; An, J.; Liu, Z. Co-simulation of dynamic underground heat transfer with building energy modeling based on equivalent slab method. *Energy Build.* **2022**, *256*, 111728. [[CrossRef](#)]
31. Shafagh, I.; Rees, S. Foundation wall heat exchanger model and validation study. In Proceedings of the IGSHPA Research Track, Orlando, FL, USA, 27–29 March 2018. [[CrossRef](#)]
32. Pokorska-Silva, I.; Kadela, M.; Fedorowicz, L. A reliable numerical model for assessing the thermal behavior of a dome building. *J. Build. Eng.* **2020**, *32*, 101706. [[CrossRef](#)]
33. Christodoulides, P.; Vieira, A.; Lenart, S.; Maranha, J.; Vidmar, G.; Popov, R.; Georgiev, A.; Aresti, L.; Florides, G. Reviewing the Modeling Aspects and Practices of Shallow Geothermal Energy Systems. *Energies* **2020**, *13*, 4273. [[CrossRef](#)]
34. Delsante, A.E.; Stokes, A.N.; Walsh, P.J. Application of Fourier transforms to periodic heat flow into the ground under a building. *Int. J. Heat Mass Transf.* **1983**, *26*, 121–132. [[CrossRef](#)]
35. Xie, X.; Jiang, Y.; Xia, J. A new approach to compute heat transfer of ground-coupled envelope in building thermal simulation software. *Energy Build.* **2008**, *40*, 476–485. [[CrossRef](#)]
36. Chen, D. Heat Loss Via Concrete Slab Floors with External Vertical Edge Insulations. *Heat Transf. Eng.* **2020**, *41*, 800–813. [[CrossRef](#)]
37. Caridad, V.; Ortiz de Zárate, J.M.; Khayet, M.; Legido, J.L. Thermal conductivity and density of clay pastes at various water contents for pelotherapy use. *Appl. Clay Sci.* **2014**, *93–94*, 23–27. [[CrossRef](#)]
38. Oyeyemi, K.D.; Sanuade, O.A.; Oladunjoye, M.A.; Aizebeokhai, A.P.; Oloajo, A.A.; Fatoba, J.O.; Olofinnade, O.M.; Ayara, W.A.; Oladapo, O. Data on the thermal properties of soil and its moisture content. *Data Brief* **2018**, *17*, 900–906. [[CrossRef](#)]

**Disclaimer/Publisher’s Note:** The statements, opinions and data contained in all publications are solely those of the individual author(s) and contributor(s) and not of MDPI and/or the editor(s). MDPI and/or the editor(s) disclaim responsibility for any injury to people or property resulting from any ideas, methods, instructions or products referred to in the content.